

The AAPM/RSNA Physics Tutorial for Residents

Radiation Detectors in Nuclear Medicine¹

Nicole T. Ranger, MSc

LEARNING OBJECTIVES

After reading this article and taking the test, the reader will be able to:

- Describe the physical process of radiation detection and the components of each detector stage.
- Define the terms *efficiency*, *energy resolution*, *energy discrimination*, and *dead time*.
- List and compare the different categories of radiation detectors.
- Describe the characteristics and function of each of the radiation detection devices found in the clinical nuclear medicine setting.

Single-photon-emitting or positron-emitting radionuclides employed in nuclear medicine are detected by using sophisticated imaging devices, whereas simpler detection devices are used to quantify activity for the following applications: measuring doses of radiopharmaceuticals, performing radiotracer bioassays, and monitoring and controlling radiation risk in the clinical environment. Detectors are categorized in terms of function, the physical state of the transducer, or the mode of operation. The performance of a detector is described by the parameters efficiency, energy resolution and discrimination, and dead time. A detector may be used to detect single events (pulse mode) or to measure the rate of energy deposition (current mode). Some detectors are operated as simple counting systems by using a single-channel pulse height analyzer to discriminate against background or other extraneous events. Other detectors are operated as spectrometers and use a multichannel analyzer to form an energy spectrum. The types of detectors encountered in nuclear medicine are gas-filled detectors, scintillation detectors, and semiconductor detectors. The ionization detector, Geiger-Müller detector, extremity and area monitor, dose calibrator, well counter, thyroid uptake probe, Anger scintillation camera, positron emission tomographic scanner, solid-state personnel dosimeter, and intraoperative probe are examples of detectors used in clinical nuclear medicine practice.

Abbreviations: FWHM = full width at half maximum, PET = positron emission tomography, SPECT = single photon emission computed tomography

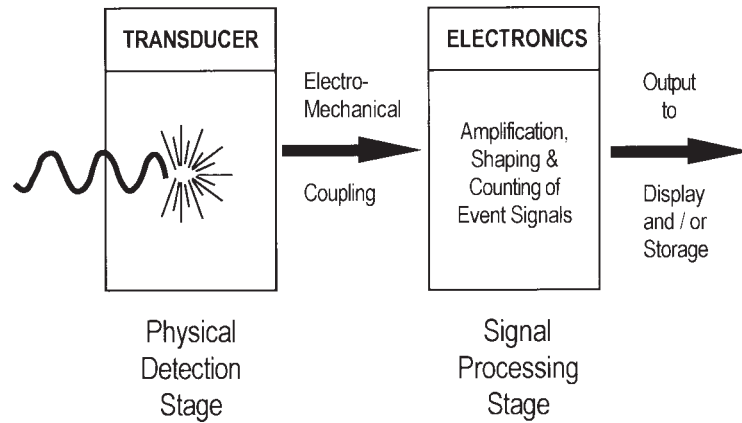
Index terms: Physics • Radiations, measurement • Radionuclide imaging

RadioGraphics 1999; 19:481-502

¹From the Department of Radiology, School of Medicine, State University of New York, Rm 092, L4 HSC, Nichols Rd, Stony Brook, NY 11794-8420. From the AAPM/RSNA Physics Tutorial at the 1997 RSNA scientific assembly. Received October 30, 1998; revision requested December 14 and received January 26, 1999; accepted January 27. **Address reprint requests to the author.**

©RSNA, 1999

Figure 1. Diagram shows the stages of radiation detection. Radiation interacts in the transducer, depositing energy by exciting or ionizing transducer atoms. The transducer is physically coupled to an electronic stage, where the subtle effect within the transducer is converted into a measurable electronic signal. The output from the electronic stage is fed into a display or storage device for interpretation.



■ INTRODUCTION

An understanding of the principles of radiation detection and the characteristics of commonly encountered detection devices is essential for the nuclear medicine practitioner. Radiation detectors can be categorized in terms of function, the physical state of the transducer, or the mode of operation.

In this article, the properties of ideal detectors are reviewed; the physical and electronic stages of detection are discussed; and gas-filled, scintillation, and semiconductor detectors are described.

■ PROPERTIES OF IDEAL DETECTORS

All radiation detectors share the characteristic that radiation incident on the transducer, the radiation-sensitive region of the detector, produces excitation or ionization effects that are not directly observable. The physical state and density of the transducer determine whether ion pair (electron-hole) formation or excitation is favored. The transducer is physically coupled to an electronic stage, where the subtle physical manifestation in the transducer is converted into a useful electronic signal, which is processed, analyzed, and counted (Fig 1).

The ideal radiation detector achieves a high absolute detection efficiency (or quantum detection efficiency) by effectively absorbing the radiation of interest. This process requires that particulate or electromagnetic radiation be able to penetrate the detector to deposit energy in the transducer and that the transducer have sufficient stopping power to absorb and therefore

detect the radiation. Maximum detection efficiency is achieved when the transducer is optimally positioned relative to the radiation source.

The performance of a detector is also characterized by the electronic stage and mode of operation. When activity levels exceed a certain limit, many detectors suffer from counting rate losses, which cause a decrease in or underestimate of the measured activity level. For efficient operation and to accurately quantitate radiation risk, it is essential that the detector have a linear response with increasing activity; such a response implies minimal or small counting rate losses or dead time at the highest counting rates encountered clinically.

In some applications, it is necessary to measure the energy of the radiation being detected by using a category of detectors called spectrometers. A pulse height spectrum (a frequency distribution of pulse heights) can be used to identify the source of the radiation and to restrict or discriminate which events will be accepted. The ability of a detection system to accurately represent deposited energy is measurable and is termed the *energy resolution*. The ideal detection system will have very good energy resolution, which implies that the detector is better able to represent, resolve, and discriminate different radiation energies.

● Absolute Efficiency

Absolute efficiency is defined as the number of radiation events detected in a given interval divided by the number of radiation quanta (particles or photons) emitted by a radiation source in the same interval. Radiation is emitted isotropically, and only a small fraction of events im-

Table 1
Stopping Powers of Various Transducer Materials

Transducer Material	Thickness (cm)	Density (g/cm ³)	Z _{eff} [*]	Linear Attenuation Coefficient μ (cm ⁻¹) by Photon Energy		
				140 keV	364 keV	511 keV
Air	1.0	0.0012	7.8	0.00017	0.00012	0.00010
Water	1.0	1.00	7.5	0.155	0.111	0.096
Thallium-activated sodium iodide	1.0	3.67	50	4.494	0.727	0.504
Bismuth germinate	1.0	7.13	74	12.950	1.650	0.920
Germanium	1.0	5.32	32	1.649	0.534	0.433
Cadmium telluride	1.0	6.20	50	5.084	0.818	0.563

*Effective atomic number.

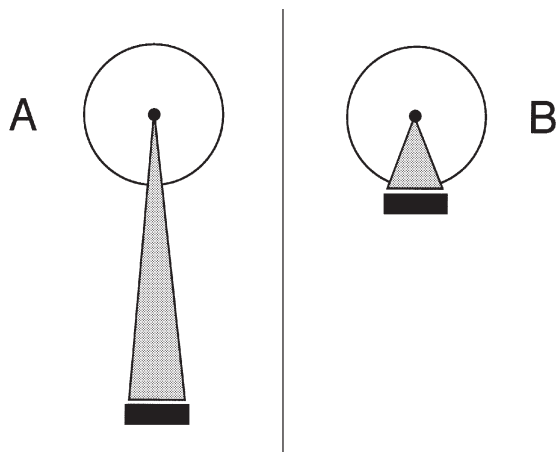


Figure 2. Diagram shows the strong correlation between source-to-detector distance and geometric efficiency. Only a fraction of the radiation emitted isotropically from a point source is incident on the detector. A comparison of A and B demonstrates that the geometric efficiency of the detector decreases with increasing source-to-detector distance in accordance with the inverse square law.

pinge on the detector (Fig 2). Of those events striking the detector, a fraction interact in the transducer, whereas the rest are absorbed before reaching the transducer or pass unimpeded through the transducer and are not detected. Therefore, the overall efficiency of the detector is determined by two factors: the intrinsic stopping power of the transducer and the spatial orientation of the detector relative to the radiation source. Absolute efficiency is more precisely defined as the product of the intrinsic and geometric efficiencies:

$$\epsilon_{\text{abs}} = \epsilon_{\text{intrinsic}} \times \epsilon_{\text{geom}}, \quad (1)$$

where $\epsilon_{\text{intrinsic}}$ is the intrinsic efficiency and ϵ_{geom} is the geometric efficiency. Both intrinsic efficiency and geometric efficiency are reported as fractions; therefore, the absolute efficiency is always less than 1.

● Intrinsic Efficiency

Intrinsic efficiency is defined as the number of events detected in a given interval divided by the number of radiation quanta (particles or photons) incident on the detector in the same interval. The intrinsic efficiency is determined by the stopping power of the transducer for the radiation of interest. The stopping power for a particular radiation is determined by the thickness, density, and atomic number of the detector. The intrinsic efficiency for detection of gamma photons is the interaction probability given by the following equation:

$$P_{\gamma} = 1 - e^{-\mu x}, \quad (2)$$

where the linear attenuation coefficient μ is a function of the density and atomic number of the material and the photon energy of interest. The linear attenuation coefficients for detection of gamma photons with various transducer materials are shown in Table 1. Intrinsic efficiency decreases with increasing photon energy and increases with increasing density. Bismuth germinate has a greater stopping power than thallium-activated sodium iodide; for this reason, bismuth germinate is favored for imaging 511-keV annihilation photons in positron emission tomography (PET) applications.

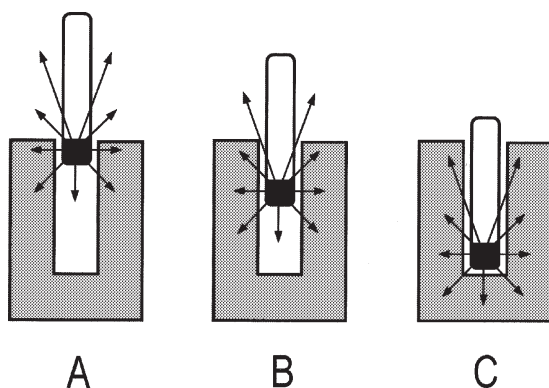


Figure 3. Diagram of the geometry of a well detector shows the effects of sample positioning. The geometric efficiency is approximately 50% in *A* but increases to more than 90% when the source is positioned at the bottom of the well, as shown in *C*.

Although intrinsic efficiency is primarily determined by the stopping power, the housing of the detector must also be designed to allow nonpenetrating radiations to enter the transducer without first being absorbed. This result is often achieved by means of a thin entrance window, which minimizes the likelihood of particulate radiation (ie, low-energy beta particles) being absorbed before detection in the transducer.

● Geometric Efficiency

Geometric efficiency is defined as the number of radiation quanta (particles or photons) incident on the detector in a given interval divided by the number emitted by the radiation source in the same interval. For a point source detected by a simple cylindrical detector (shown in cross section in Fig 2), the geometric efficiency decreases with increasing source-to-detector distance in accordance with the inverse square law. In some applications that require more sensitivity and accuracy, the detector may be designed to almost completely surround the source. Such is the case with the scintillation well counter, which is designed for maximum detection efficiency due to the low levels of activity found in bioassay samples. Even with these design considerations, if a source sample is not positioned properly in a well detector, the overall efficiency will be significantly decreased (Fig 3).

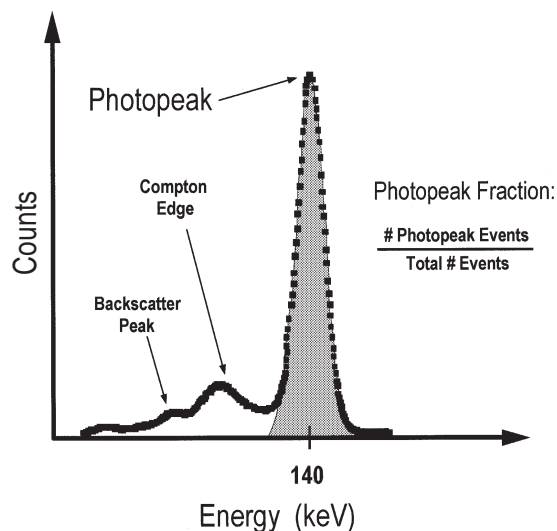


Figure 4. Diagram of an energy spectrum for Tc-99m shows the characteristic photopeak at 140 keV. The photopeak fraction is defined as the ratio of photopeak events to total events.

● Energy Resolution

For the class of radiation detectors called spectrometers, the ability to accurately represent the energy of the radiation event being detected is an essential requirement. When a scintillation detector operated as a spectrometer is irradiated with a monoenergetic beam of gamma photons, the output of the spectrometer is a series of voltage pulses. The amplitude of these voltage pulses is proportional to the energy deposited in the detector; when the pulses are sorted by amplitude, the result is a pulse height distribution or energy spectrum. An energy spectrum from a scintillation camera irradiated with a point source of technetium-99m is shown in Figure 4. The distribution of measured energies arises because of the following limitations in the detection process and other physical phenomena: (a) photoelectric interactions in which all of the photon energy is deposited in the detector and (b) Compton scattering out of and into the detector. The photopeak is the defining feature of the spectrum because it characterizes the photon energy being detected. The photopeak fraction is defined as the number of photopeak events divided by the total number of events.

The breadth of the photopeak is an indication of the ability of the detector to accurately represent detected energy. The narrower the

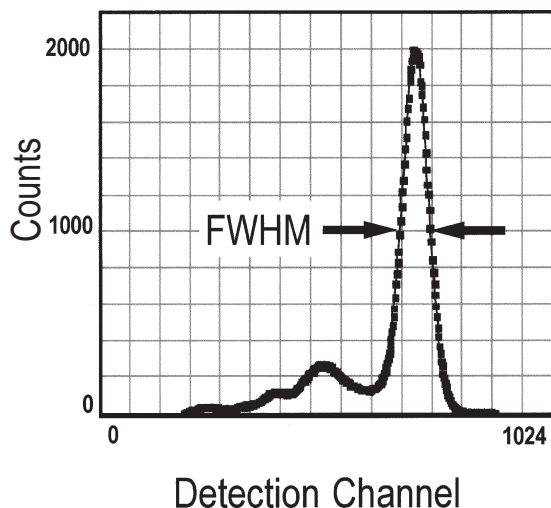


Figure 5. Diagram of an energy spectrum shows estimation of the energy resolution from the width of the photopeak. The width of the photopeak gives an indication of the magnitude of the uncertainty in the measured energy for individual events. The FWHM is measured at exactly one-half of the maximum value of the photopeak. Energy resolution is defined as the FWHM divided by the photopeak energy and is expressed as a percentage (see Eq [3]).

photopeak breadth, the better the ability of the detector to represent the energy of the radiation being detected. The energy resolution of the detector is determined by measuring the width of the photopeak at exactly one-half of the height, a measurement termed the *full width at half maximum* (FWHM) (Fig 5). Energy resolution is usually represented as a fractional percentage and is given by the following equation:

$$\text{FWHM/PE} \times 100\%, \quad (3)$$

where FWHM is in kilo electron volts and PE is the photopeak energy in kilo electron volts. (FWHM and photopeak energy are channel values, which are converted into energy with the calibration factor in Eq [4].)

Uncalibrated energy channel values are converted into kilo electron volts with a channel-to-kilo electron volt conversion factor, which is determined from a comparison of the photopeak energies and channel locations close to the energy of interest (ie, Tc-99m [140 keV] and cobalt-57 [122 keV]). This conversion factor is calculated with the following equation:

$$\left| \frac{\text{Photopeak 1} - \text{Photopeak 2}}{\text{Peak 1 Channel} - \text{Peak 2 Channel}} \right|, \quad (4)$$

where the photopeaks are in kilo electron volts. A linear relationship between channel position and energy is assumed.

A number of factors affect energy resolution. The size, thickness, and state of the transducer; the photon energy; and the characteristics of the electronic stage all determine the limits of energy resolution. The energy resolution of a conventional scintillation camera with a $\frac{3}{8}$ -inch (0.95-cm) thallium-activated sodium iodide crystal is currently 9%-10% at 140 keV. As the quantum detection efficiency is increased by detection of higher-energy photons, energy resolution is improved as a result of an increase in the number of photons emitted in the scintillation process, thereby reducing the statistical variation in measured photon energies. However, the improvement in energy resolution with higher-energy photons is offset by a decrease in stopping power and a corresponding decrease in detection efficiency at increasing photon energies.

● Dead Time

The characteristics of a detector are strongly influenced by the details of the electronic stage of the detector. There are two basic categories of electronic operation: pulse mode and current mode. In pulse mode operation, each individual event is processed separately. For most detectors operated in pulse mode, the resulting event pulse height is proportional to the energy deposited by the incident radiation. (The Geiger-Müller detector is a notable exception.) The pulse duration or electronic dead time limits the rate of detection because each pulse must be processed individually. Detection systems operated in this mode are used in low-counting rate applications for this reason.

In current mode operation, there is continuous charge collection, which results in the loss of information for individual events. The amplitude of the signal generated is proportional to the rate of energy deposition or dose rate and represents the total energy being detected in a given interval. Detectors operated in this mode are less susceptible to dead time effects; however, because individual events are not being processed, the energy of individual radiation particles or photons being detected cannot be measured.

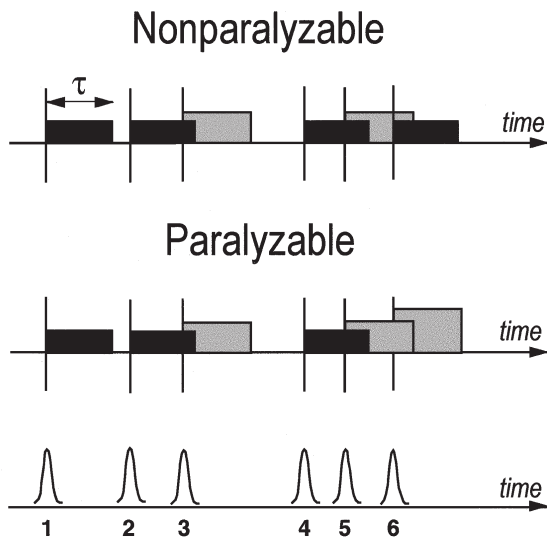
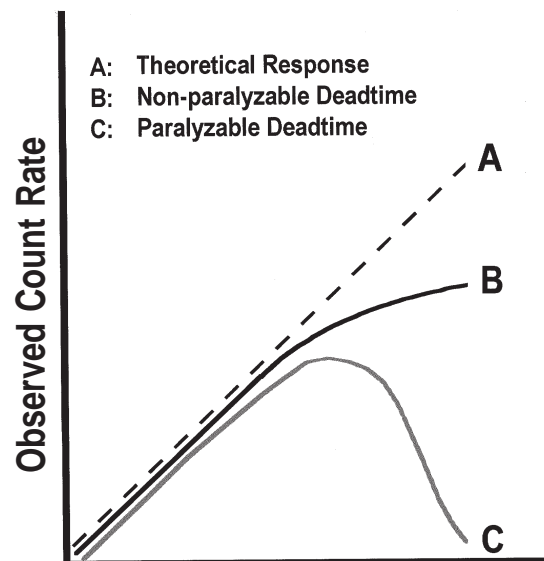


Figure 6. Diagram shows two categories of dead time. Black bars = processed events, gray bars = non-processed events. In a system with nonparalyzable dead time, events that arrive before complete processing of earlier events are rejected (events 3 and 5). In a system with paralyzable dead time, the usual dead time effect is experienced; however, the arrival of a secondary event extends the dead time, causing the secondary event to be rejected. This feature is demonstrated by the rejection of event 6 in addition to events 3 and 5.

When systems are operated in pulse mode, radiation events separated by an interval greater than the dead time τ are successfully processed and are recorded (Fig 6). If event rates increase to the extent that pulses start to overlap or pile up, the effect on detection efficiency can be marked. Detection systems are characterized by the response to high counting rates. Nonparalyzable systems will reject a second pulse that arrives before the first event is fully processed. In paralyzable systems, not only is the second event rejected, but rejection of this event extends the dead time so that a third event arriving before completion of processing is also rejected.

In an ideal detection system, which does not experience any dead time, a linear relationship would be expected when the observed or measured counting rate is plotted against the true or expected counting rate. However, in nonparalyzable systems, as the rate of events striking the detector increases, we see a corresponding

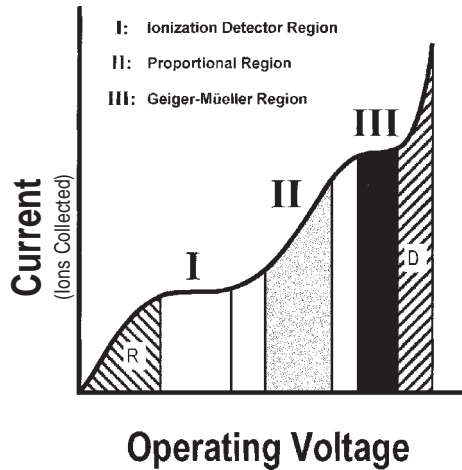
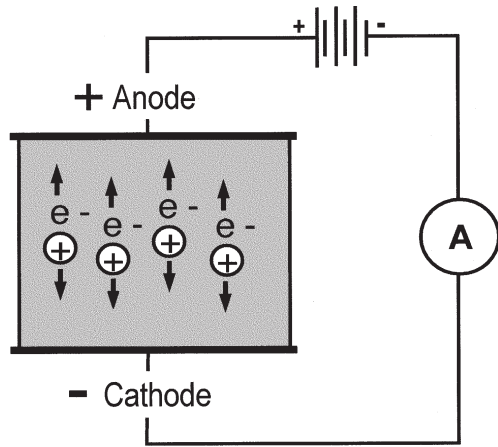


Input Count Rate

Figure 7. Diagram shows the effects of dead time on counting efficiency. *A* is the response of an ideal detection system: a straight line with a slope of 1. *B* is the response of a nonparalyzable system. The dead time increases with increasing counting rates, an effect that results in significant counting losses and counting rate saturation in the plateau region. *C* is the response of a paralyzable system. Saturation is again experienced; however, as the input rates increase beyond the saturation region, the system becomes paralyzed. The result is a rapid loss of detection efficiency beyond the saturation region.

decrease in the observed counting rate. At some point, regardless of how high the event rate increases, the observed rate reaches a maximum and does not increase further. This point is the area of plateau shown in Figure 7. In paralyzable systems, the observed rate also reaches a maximum at some event rate. However, beyond this saturation point, the observed rate decreases rapidly as the system becomes essentially paralyzed due to an inability to process events at these high rates.

The scintillation camera is an example of a detection device that experiences paralyzable dead time. A 1-mCi (37-MBq) Tc-99m point source moved toward an uncollimated detector produces observed counting rates that slowly increase, reach a plateau, and then decrease significantly as the system becomes paralyzed.



8.

9.

Figures 8, 9. (8) Diagram shows a simple schematic of a gas-filled detector. Radiation interacts in the transducer, which is filled with air or pressurized gas. Ion pairs are collected by applying a voltage across two electrodes. The electrons migrate to and are collected at the anode, whereas the positive ions are collected at the cathode to generate a current detected by a current-measuring device (A). The amplitude of the resulting current is proportional to the number of ion pairs collected but not necessarily to the number of ion pairs formed (see Fig 9). (9) Diagram shows the relationship between ion collection or current and operating voltage. Ion pairs produced in the first region (R) are not completely collected due to ion pair recombination. As the voltage is increased, a saturation point is reached where all ions are collected and the current is constant over a limited voltage range. In the ionization region (I), ion collection is proportional to the energy deposited in the detector. As the voltage is increased further, ion pairs start to gain sufficient kinetic energy to induce secondary ionization, which produces an amplification effect. This effect occurs in the proportional region (II). As the voltage is increased further still, there is a massive amplification effect such that the number of ion pairs formed is independent of the energy of the radiation interacting in the detector. This region of plateau is the Geiger-Müller region (III), where the detector is operating at maximum sensitivity. Beyond the Geiger-Müller region is a region (D) where the applied voltage causes spontaneous discharge.

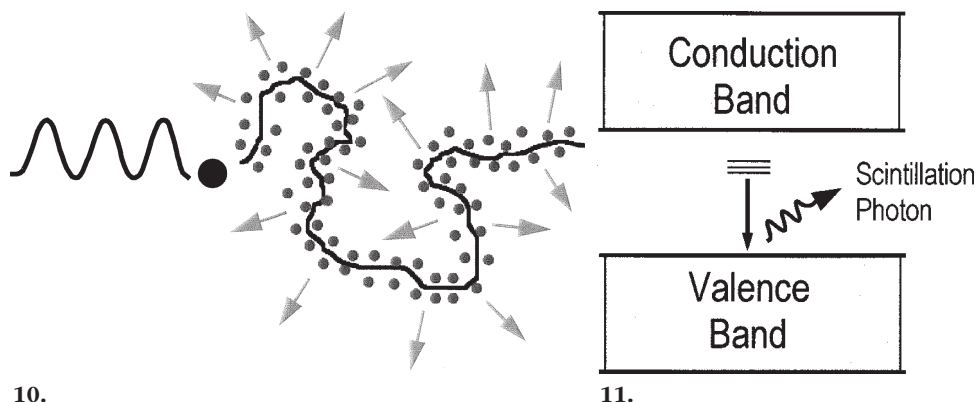
■ THE PHYSICAL STAGE

● Physics of Gas-filled Detectors

In gas-filled detectors, gas trapped in a containment vessel functions as the transducer. Radiation interacting within the gas ionizes gas atoms, and the resulting positive gas ion and free electron are termed an *ion pair*. The average energy required to produce an ion pair in air is 33 eV. If the energy from a 140-keV gamma ray was completely deposited in the detector, we would expect approximately 4,200 ion pairs to be formed versus approximately 15,500 for a 511-keV gamma ray. To measure the magnitude of the energy deposited in the detector, the ion pairs produced are collected by applying a voltage across two collecting electrodes (Fig 8). When the ions are collected, a current is generated, the magnitude of which is related to the rate of ion collection.

The number of primary ion pairs originally produced is proportional to the energy deposited in the detector but is not necessarily equivalent to the number of ions collected. There are two reasons for this outcome: (a) Not all primary ions are collected and (b) secondary ionization (and ion pair production) can occur under some operating conditions.

When ion collection is plotted versus applied voltage, a characteristic response is seen (Fig 9). In the first region of this plot, recombination of ion pairs competes with collection; however, ion collection steadily increases with the applied voltage until a saturation voltage that corresponds to maximum ion collection is reached.



10.

11.

Figures 10, 11. (10) Diagram shows an expanded view of radiation interaction in a scintillation crystal. A fast electron (●) produced as a result of Compton or photoelectric interaction travels a convoluted path and excites additional electrons (•). In a scintillator doped with activator atoms, these electrons lose excitation energy by emitting light photons (arrows). Wavy line = gamma ray. (11) Diagram shows modification of the band structure of a scintillator by the addition of activator atoms or impurities. Ionizing radiation causes excitation, which causes electrons to migrate to and become trapped at activation sites within the crystal. When the electrons return to the ground state, excitation energy is released in the form of a scintillation photon.

Beyond the saturation voltage is a plateau where all primary ions have been collected and the detector response is stable across a wide voltage range. These features make it possible to determine with reasonable accuracy the energy deposited by radiation interacting in the detector. This region is termed the *ionization region*, and gas-filled detectors operated in this mode are termed *ionization detectors*.

As the voltage is increased beyond the ionization region, electrons being accelerated gain sufficient kinetic energy that they in turn induce secondary ionization and ion pairs, which are also collected. This gas amplification effect increases with increasing voltage in the next region, which is termed the *proportional region*. The magnitude of charge collection is 100,000 times greater for proportional counters than for ionization detectors; this feature makes proportional counters useful in area monitoring and other low-level radiation monitoring applications. Nevertheless, the proportional counter is not routinely encountered in the clinical nuclear medicine setting.

When the voltage is increased further still, beyond the proportional region, the gas amplification effect increases more and more until a saturation region is reached where ion collection does not increase further with increasing voltage. In this region, which is termed the *Geiger-Müller region*, the number of ion pairs collected from each radiation event is approximately the same regardless of the energy of the radiation producing the event. The magnitude

of charge collection is very high, and billions of ion pairs are produced per event. Because of this sensitivity, the Geiger-Müller detector is very useful for low-level radiation surveying; however, the relatively long dead time precludes use of the Geiger-Müller detector in very high radiation fields.

Beyond the Geiger-Müller region is the region of continuous discharge, where ionization occurs spontaneously independent of radiation-induced ionization. Operation in this region would render the detector useless and potentially induce permanent damage. For this reason, detectors are not operated at voltages beyond those encountered in the Geiger-Müller region.

● Physics of Scintillation Detectors

A class of materials called scintillators release visible or ultraviolet light when radiation interacting within them deposits energy by means of a Compton or photoelectric interaction. Although scintillators may be liquid or crystalline, the most prevalent scintillator in nuclear medicine is the scintillation crystal. A fast electron produced as a result of a Compton or photoelectric interaction in the scintillation crystal travels a convoluted path and excites additional electrons along its trajectory (Fig 10). In a crystal that has been doped with a very small fraction of activator atoms or impurities, the excited electrons migrate to and become trapped at the activation sites where the band structure of the crystal has been modified. These electrons lose energy and thereby cause emission of light photons (Fig 11).

Table 2
Characteristics of Scintillation Crystals Most Commonly Encountered in Nuclear Medicine

Scintillation Crystal	Decay Constant (μsec)	Density (g/cm^3)	Z_{eff}^*	Conversion Efficiency (%) [†]
Thallium-activated sodium iodide	0.230	3.67	50	100
Bismuth germinate	0.300	7.13	74	12-14

*Effective atomic number.

†Relative to that of thallium-activated sodium iodide.

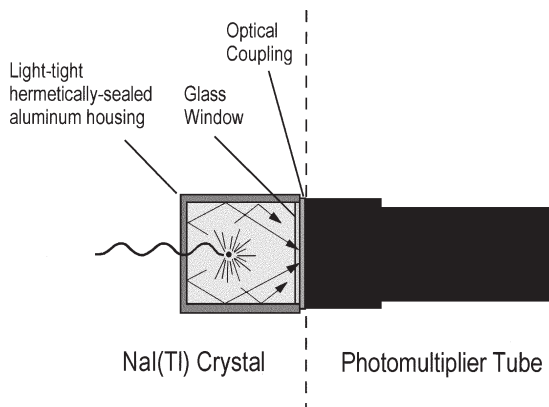


Figure 12. Diagram shows a scintillation detector that consists of a thallium-activated sodium iodide crystal coupled to a photomultiplier tube. A radiation interaction in the crystal produces a flash of light, which is emitted isotropically from the point of interaction. The number of scintillation photons produced is proportional to the energy deposited. Light is collected by the photomultiplier, where it is converted into an electric signal. The crystal has a reflective coating so that scintillation photons are ultimately reflected toward the glass exit window and into the photomultiplier. Maximum light transmission with minimum light spreading is achieved by optically coupling the crystal to the photomultiplier.

The most commonly encountered scintillation crystal in nuclear medicine is thallium-activated sodium iodide. Thallium-activated sodium iodide has an emission spectrum of 315-550 nm (blue light region) with a peak at 415 nm, which corresponds to a photon energy of approximately 3 eV. The scintillation efficiency of a scintillator is defined as the fraction of deposited energy that is converted into light. If a scintillation efficiency of 12% is assumed and the energy from a 140-keV photon is completely deposited in a thallium-activated sodium iodide crystal by means of a photoelectric interaction, approximately 5,600 light photons would be emitted isotropically from the

point of interaction. Even though the absolute scintillation efficiency of thallium-activated sodium iodide is only 12%, this scintillator has a high conversion efficiency compared with that of bismuth germinate (Table 2). This fact contributes to the relatively high energy resolution of thallium-activated sodium iodide, which also has a shorter decay constant than bismuth germinate and is the scintillator of choice for nuclear medicine counting and imaging applications. Bismuth germinate has a higher stopping power and is favored for PET applications.

● The Scintillation Detector

Sodium iodide is the crystal most often used in the scintillation detectors used in nuclear medicine. A schematic of a typical thallium-activated sodium iodide crystal and photomultiplier tube is shown in Figure 12. A thallium-activated sodium iodide crystal is formed by adding trace amounts of thallium to a pure sodium iodide crystal during growth. Sodium iodide crystals are hygroscopic and must be sealed in an air-tight enclosure to avoid absorption of moisture from exposure to air. Crystals that have been exposed to air for any length of time lose the properties of transparency and light transmission and are said to be "yellowed." The crystal is covered with a highly reflective coating so that light photons emitted in directions other than toward the exit window are eventually reflected out the window to the photomultiplier, the device that converts the light photons into an electric signal. The exit window of the crystal is constructed of highly polished glass, which is coupled to the photomultiplier with optical gel or epoxy. This optical coupling is required to match the indexes of refraction of the exit window of the crystal to the entrance window of the photomultiplier to maximize light transmission and minimize light refraction or spreading.

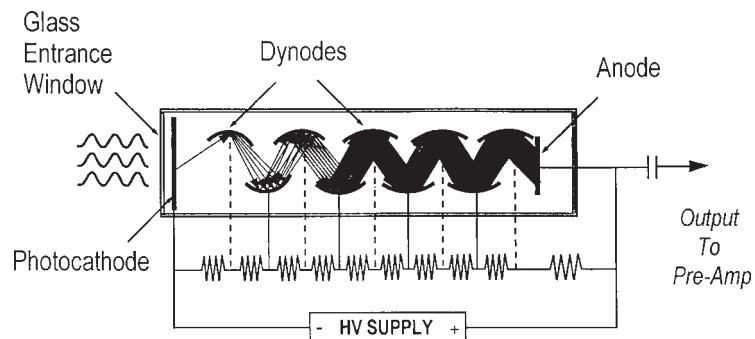


Figure 13. Diagram shows a schematic of a photomultiplier. Light photons entering the glass entrance window impinge on the photocathode; the result is emission of one electron for approximately every five light photons. The electron produced is accelerated toward a dynode chain. The accelerated electron has sufficient kinetic energy to liberate approximately five additional electrons when it strikes each dynode. The effective electron gain at the collecting anode is 10^6 to 10^8 . The output of the photomultiplier is a signal with a characteristic shape (see Fig 17); the amplitude of this signal is proportional to the number of photons entering the photomultiplier or the energy deposited in the crystal. *HV* = high voltage, *Pre-Amp* = preamplifier.

The photomultiplier (shown schematically in Fig 13) converts light emitted from the crystal into a useful electric signal. The photomultiplier is chosen to have a spectral sensitivity that closely matches the spectral output of the scintillation crystal to which it is coupled. Just inside the entrance window of the photomultiplier is the photocathode, an electrode coated with photosensitive material. On average, for every five scintillation photons striking the photocathode, one electron is emitted. The electron produced is then accelerated toward an electron multiplier system consisting of 10 or so specialized electrodes called dynodes. Each dynode is at approximately 100 V higher potential than the preceding dynode. As electrons are accelerated toward each dynode, they gain sufficient kinetic energy to eject several electrons at impact. If five electrons are ejected at each dynode and the photomultiplier has N dynodes, then the total number of electrons collected at the anode for each emitted from the photocathode is 5^N . This process produces an electron gain that is usually on the order of 10^6 to 10^8 . The overall response of the photomultiplier is linear because the output signal is proportional to the number of light photons striking the pho-

tocathode; the number of light photons striking the photocathode is in turn proportional to the total energy deposited in the crystal. This characteristic is exploited in the scintillation camera, where all photomultiplier signal outputs are summed to create a "Z" signal that is representative of the total energy deposited in the detector.

A comparison of scintillators is presented in Table 2. Conventional scintillation cameras use a large-area thallium-activated sodium iodide crystal, whereas dedicated PET devices predominantly use bismuth germinate crystals because of the improved stopping power of bismuth germinate at 511 keV.

● Physics of Semiconductor Detectors

The laws of physics dictate that there are only certain allowed energy states for electrons in solids. For the class of detectors called solid-state detectors, this fact is significant because charge carriers must be collected directly, whereas scintillation photons travel unimpeded through a scintillation crystal.

There are two energy band states for electrons in solids: the valence band, which represents the range of energies for bound electrons, and the conduction band, which represents the range of energies for unbound electrons (Fig 14). Between these two states is a forbidden energy

A: Insulator

B: Semiconductor

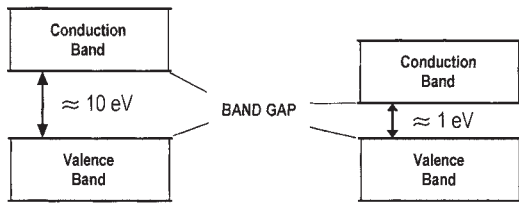


Figure 14. Diagram shows the allowed energy states for electrons in solids. The valence band represents energy states for bound electrons. The conduction band represents energy states for unbound electrons. The band gap is the zone representing forbidden energy states between these regions. The band gap energy is the energy required to move an electron from the valence band to the conduction band and is a factor of 10 less for semiconductors than for insulators.

Table 3
Band Gap Energies for Various Semiconductor Materials

Semiconductor Material	Band Gap Energy (eV)
Germanium	0.72
Silicon	1.10
Gallium arsenide	1.42
Cadmium telluride	1.47

zone called the band gap region. The band gap represents the energy barrier that must be overcome to move an electron from the valence band to the conduction band or, more simply, to free an electron from the binding energy. The band gap for insulators is on the order of 10 eV, whereas the band gap for semiconductor materials is closer to 1 eV.

The band gap represents an energy threshold for electron mobility, and this feature is exploited when semiconductors are used as radiation detectors: Electrons are raised to the conduction band when radiation interacts and deposits energy in the detector. Many semiconductor detectors require cooling to sufficiently low temperatures that electrons are not elevated to the conduction band by thermal energy. Two intrinsic semiconductors that require cooling with liquid nitrogen are germanium and silicon, which have band gap energies of 0.72 eV and 1.10 eV, respectively (Table 3). Gallium arsenide and cadmium telluride semiconductors have

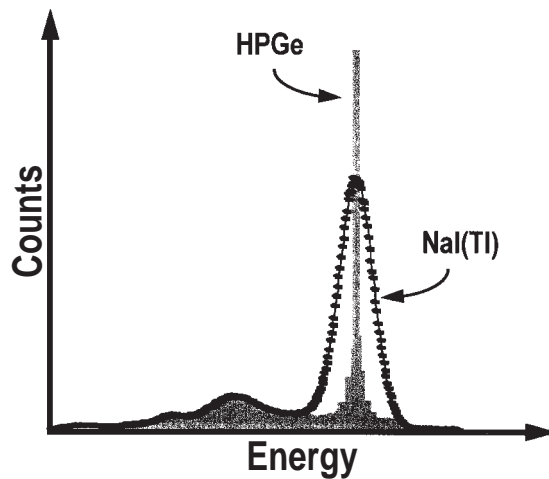


Figure 15. Diagram shows the energy spectra of high-purity germanium (HPGe) and thallium-activated sodium iodide (NaI(Tl)) for Tc-99m. The improved energy resolution and efficiency of the high-purity germanium detector are clearly demonstrated.

band gap energies of 1.42 eV and 1.47 eV, respectively, which are sufficiently high that these semiconductors can be operated at normal room temperatures.

● **High-Purity Germanium Detector**

An example of an intrinsic semiconductor is the high-purity germanium detector, which must be cooled with liquid nitrogen to 77 K (-196°C), the normal operating temperature. This detector has a relatively high density, which makes it efficient for the detection of x rays and gamma rays. The band gap energy for high-purity germanium detectors is 0.72 eV; however, on average it takes 3 eV to create an electron-hole pair. High-purity germanium detectors have an output signal with a relatively large amplitude because the 3-eV ionization threshold is less than one-tenth of the ionization threshold for gas-filled detectors. This quantum efficiency gain translates into a significantly improved energy resolution. The energy resolution of high-purity germanium detectors is in the range of 0.3%–1.0% at 122 keV.

A comparison of the energy resolution of the high-purity germanium detector with that of the thallium-activated sodium iodide detector for 140-keV photons is presented in Figure 15.

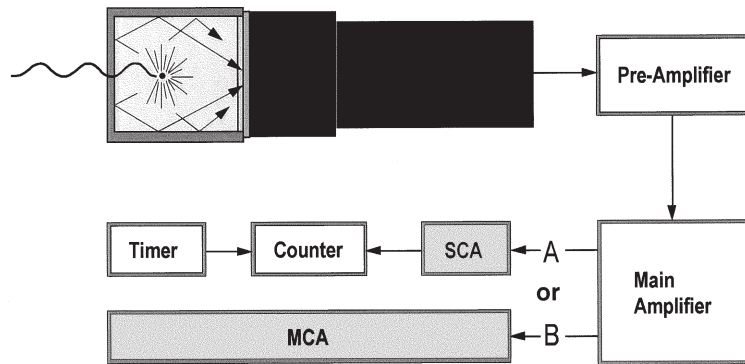


Figure 16. Diagram shows the components of the electronic stage for a scintillation detector. The stream of electrons from the photomultiplier is collected at the anode; the result is a current pulse to the pre-amplifier. The output signal from the preamplifier is fed to the main amplifier, from which the signal travels to a single-channel analyzer (SCA) for simple counting systems or to a multichannel analyzer (MCA) for detection systems operated as spectrometers.

The high resolution and relative efficiency of the high-purity germanium detector compared with those of gas-filled and scintillation detectors make it very efficient in gamma ray spectroscopy applications. Nevertheless, the high-purity germanium detector is not usually encountered in the clinical nuclear medicine setting.

■ THE ELECTRONIC STAGE

Figure 16 shows a typical representation of the electronic processing stage for a scintillation detector. The output from the photomultiplier is input to the preamplifier, which matches the impedance of the signal between the photomultiplier and amplifier stages and amplifies and shapes the signal for optimal processing. The signal is further amplified and shaped at the main amplifier, where the amplitude of the signal is increased by a factor of 1,000, from a few millivolts to a few volts. For simple counting systems, the amplitude of the signal is then evaluated by a pulse height analyzer circuit in a single-channel analyzer. The output pulses from the single-channel analyzer are counted for a set interval by a counter-timer circuit. For detection systems used as spectrometers, the output of the amplifier is input into a multichannel analyzer, where the pulse height is sampled by an analog-to-digital converter and the result is stored in memory. When a large number of events are analyzed in this way, the result is the accumulation of an energy distribution or energy spectrum that is characteristic of the radiation being detected.

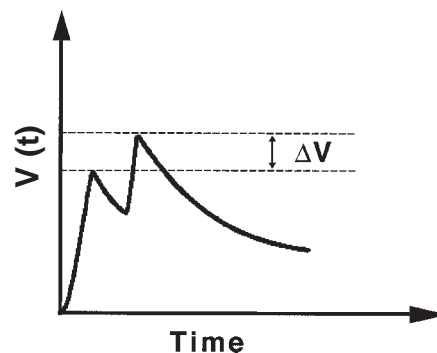
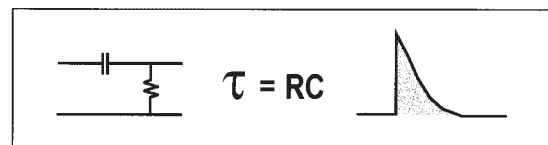


Figure 17. Diagrams show a basic preamplifier circuit and the effects of preamplifier pulse pileup. Top: For a basic preamplifier circuit, τ is the product of resistance (R) and capacitance (C). Bottom: Two events overlapping in time cause pileup of the preamplifier signal. The resulting displacement of the second signal (ΔV) introduces errors in estimating the energy of the radiation event detected. $V =$ voltage.

● Preamplifier

The functions of the preamplifier are to amplify the signal produced by the detector, to match the impedance of the signal between the detector and the amplifier, and to shape the signal for optimal processing. In the simplest configuration, the preamplifier consists of a capacitor

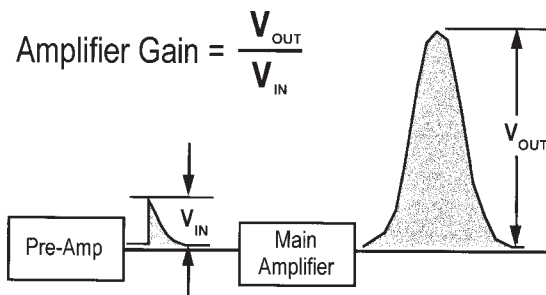


Figure 18. Diagram shows the functions of the main amplifier. The preamplifier (*Pre-Amp*) signal V_{IN} is fed to the main amplifier. The result is a shaped, symmetric signal with amplitude V_{OUT} . The amplifier gain is the ratio of V_{OUT} to V_{IN} .

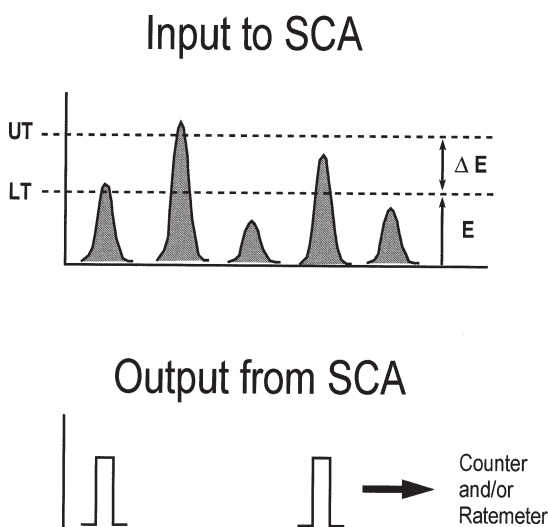


Figure 19. Diagram shows the effects of pulse height analysis in a single-channel analyzer (*SCA*). The input to the analyzer is symmetric analog voltage pulses with amplitudes proportional to the energy (E) of the detected event. A preset lower threshold (LT) and upper threshold (UT) permit simple energy discrimination. Signals with amplitudes outside the accepted range are rejected and not counted. For each accepted signal, the analyzer outputs a pulse, which is counted by the counting circuit.

and resistor circuit (Fig 17), which produces a signal with a characteristic decay time or time constant τ . The decay time is the time it takes a preamplifier signal to decay to 37% of the maximum amplitude and is defined as follows:

$$\tau = R \times C, \quad (5)$$

where R is the resistance in ohms and C is the capacitance in farads.

The result of this decay time is that a second signal arriving before the first signal has been processed induces a pulse pileup effect (Fig 17). This displacement causes the amplitude of the preamplifier signal to misrepresent the energy deposited in the detector and limits the accuracy and counting rate capability of the detection system.

In many applications, the preamplifier is found in the base of the photomultiplier. In this location, the proximity to the output of the photomultiplier minimizes electronic noise transmission and thus improves signal-to-noise characteristics.

● Amplifier

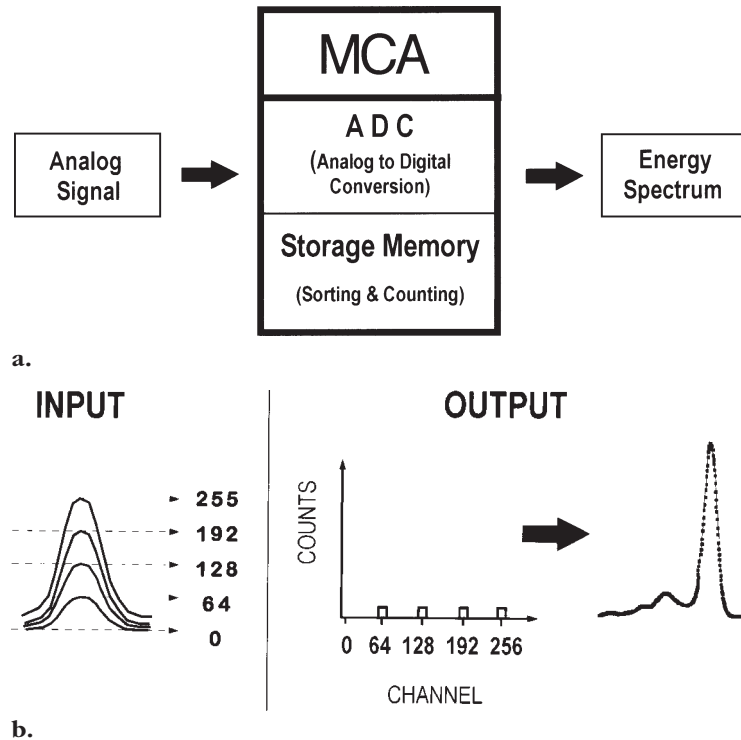
The amplifier increases the amplitude of the preamplifier signal from a few millivolts to a few volts (the amplifier gain) and converts an asymmetric input signal with a relatively long decay time into a symmetric voltage pulse, thereby improving the signal timing characteristics (Fig 18). Without this additional pulse shaping, a preamplifier output with a characteristic decay time of 500 μsec would produce pulse pileup effects at counting rates beyond 2,000 counts per second. A typical amplifier voltage gain is 1,000.

● Energy Discriminators

The output signal of the amplifier has an amplitude proportional to the energy deposited in the detector. If it is assumed that the response of the detector is linear, the relative energy of the event being detected can be estimated by performing pulse height analysis on each signal. This information can then be used to accept or reject events or, if required, to generate a histogram of measured energies from the detector. There are two classes of pulse height analyzer systems: the single-channel analyzer and the multichannel analyzer.

A single-channel analyzer is a simple pulse height analyzer in which pulses with amplitudes that correspond to the acceptable energy range are sent on to be counted, whereas pulses with amplitudes below a lower threshold or above an upper threshold are rejected (Fig 19). For accepted events, the pulses from the single-channel analyzer are all exactly the same and are output to a counter or rate meter to be tabulated.

Figure 20. (a) Diagram shows the components of a multichannel analyzer (MCA). The amplitudes of analog signals input into the analyzer are sampled by an analog-to-digital converter (ADC). The resulting amplitude information permits individual events to be characterized by the event energy. Memory locations are assigned to each energy range; as each amplitude is analyzed by the analog-to-digital converter, a memory location corresponding to that pulse height analysis range is incremented by 1. (b) Diagram shows the energy spectrum produced by accumulation and analysis of the amplitudes of input analog signals.



In a multichannel analyzer, the pulse height of each input analog signal is digitized by an analog-to-digital converter (Fig 20). The output of the analog-to-digital converter is a binary number, which gives a relative indication of the energy of the event. The multichannel analyzer tabulates the voltage pulses on the basis of the output of the analog-to-digital converter by assigning an energy range to each of the detection channels. If a voltage pulse falls within the range represented by one of the channels, a computer memory location corresponding to that channel has the number of counts in it incremented by 1. By performing this operation for all detected events in a given interval, the multichannel analyzer generates a spectrum of the distribution of energies for measured events (energy histogram) with the y axis representing counts and the x axis representing channel value (relative energy).

Figure 21a presents an example of energy discrimination by a single-channel analyzer. The lower threshold of 126 keV and upper threshold of 154 keV correspond to a 20% ($\pm 10\%$) energy window about the 140-keV photopeak of Tc-99m. An alternate representation of this energy window is shown in Figure

21b. In this example, an energy spectrum from a multichannel analyzer has the lower and upper thresholds represented as vertical lines on either side of the centroid of the photopeak. This mode of energy window display is employed on imaging devices to facilitate visual alignment of the pulse height analyzer window with the photopeak. By this means, scattered events can be selectively rejected to optimize image quality.

● Coincidence Detection

In some applications involving positron-emitting radioisotopes, it is useful to operate a detector in the coincidence detection mode. The positron is detected indirectly by detecting annihilation photons produced as a result of positron annihilation with an electron. The 511-keV gamma annihilation photons are emitted simultaneously (in coincidence) at approximately 180° to each other. Coincidence detection systems employ two opposing detectors and use a coincidence circuit to accept only those events that fall within a narrow interval or coincidence window (Fig 22), which is typically 20–50 nsec depending on the type of detector system used. The total measured coincidence counting rate consists of true coincidences and accidental or random coincidences from events that just happen to

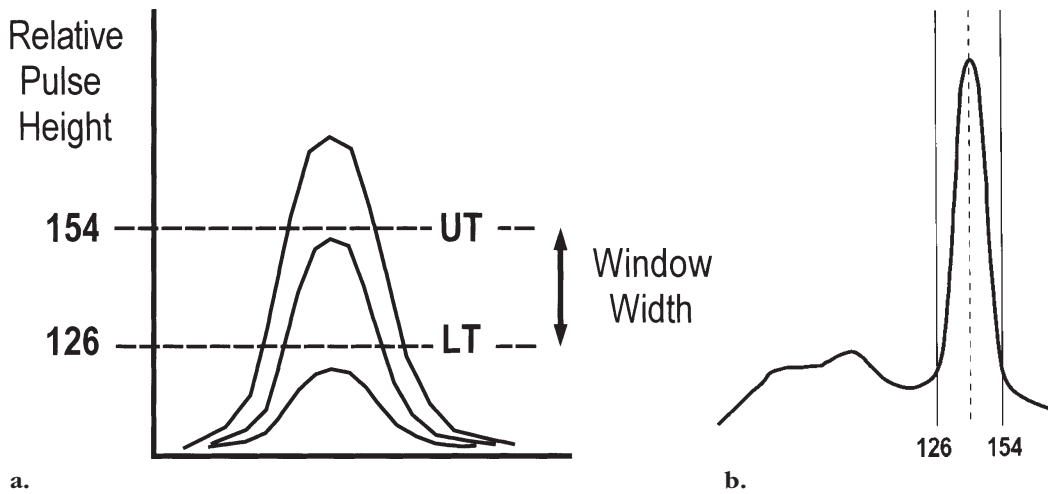


Figure 21. (a) Diagram shows the lower threshold (*LT*) and upper threshold (*UT*) of a single-channel analyzer for a 20% ($\pm 10\%$) energy window at 140 keV. (b) Diagram shows an alternate representation of the 20% energy window at 140 keV. The acceptance window of a multichannel analyzer is shown relative to the energy spectrum; the window is represented as vertical lines on either side of the photopeak that correspond to the 20% ($\pm 10\%$) limits.

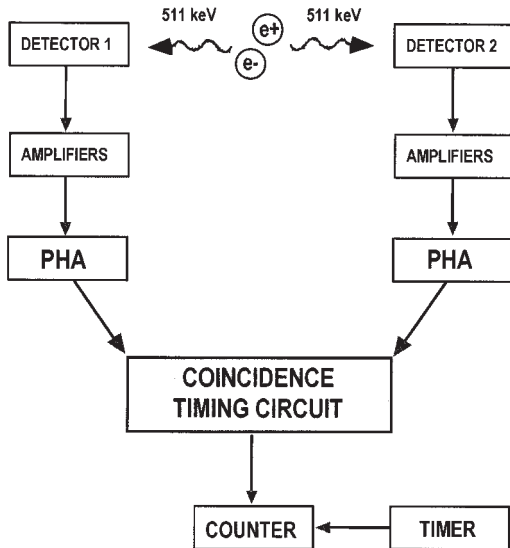


Figure 22. Diagram shows a coincidence detection circuit used for counting of a positron-emitting sample. The 511-keV annihilation photons produced are emitted at approximately 180° in coincidence and are detected by an opposing pair of detectors. After conventional pulse height analysis (*PHA*), the arrival times of detected events are compared by a coincidence timing circuit. Those events falling within a preset timing window are assumed to be coincident events and are processed, whereas all others are rejected.

arrive within the preset time window. The random counting rate is calculated as follows:

$$R = \sqrt{(S_1 S_2)}, \quad (6)$$

where *R* is the random counting rate and *S*₁ and *S*₂ are the "singles" counting rates of the detectors involved in the measurement.

Table 4
Detectors Encountered in Nuclear Medicine

Gas-filled detectors
Ionization detectors
Geiger-Müller detector
Extremity and area monitor
Dose calibrator
Scintillation detectors
Well counter
Thyroid uptake probe
Anger scintillation camera
PET scanner
Semiconductor detectors
Personnel dosimeters
Intraoperative probes
Imaging devices

Coincidence detection is employed in PET scanners used for imaging positron-emitting radionuclides and in some automatic blood sampling systems used during PET studies.

■ GAS-FILLED DETECTORS

Gas-filled detectors are almost exclusively relegated to surveying, personnel and area monitoring, and radionuclide dose quantitation. Such detectors include ionization detectors, the Geiger-Müller detector, the extremity and area monitor, and the dose calibrator. The various detectors encountered in nuclear medicine are listed in Table 4.

● Ionization Detectors

The ionization detector shown in Figure 23a is a handheld device used for radiation surveying. As with all gas-filled detectors in the ionization detector mode of operation, the rate of ion pair collection is proportional to the energy of the radiation being detected. Therefore, this device provides accurate readings of exposure when air is the transducer and exposures are in the range of 1 mR (2.58×10^{-7} C/kg) to 1 R (2.58×10^{-4} C/kg). This feature makes these survey meters very useful for accurate exposure measurements despite the relatively low sensitivity compared with that of the Geiger-Müller detector. Like all gas-filled detectors, ionization detectors are relatively inefficient for detecting x rays and gamma rays in comparison with scintillation detectors. In some gas-filled detectors, higher stopping power can be achieved by using pressurized argon or xenon gas; however, because exposure is defined only in air, air is the transducer of choice in survey instruments used to measure exposure. Ionization detectors are operated in current mode, have short dead times, and are more useful in high radiation fields than the Geiger-Müller detector.

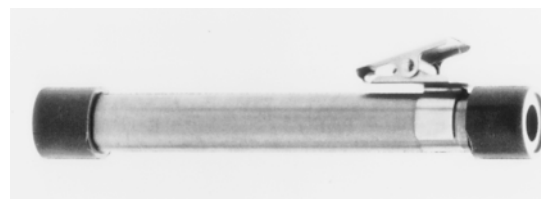
A specialized version of the ionization detector is the pocket ionization detector (Fig 23b). This device is essentially an electrometer that is calibrated to read zero when the charge is maximum on a quartz fiber mounted inside. As the sensitive volume is exposed to radiation, ion pairs collected reduce the charge on the quartz fiber; this reduction causes the fiber to deflect from the zero calibration point in proportion to the cumulative exposure. By peering through a lens at the top of the cylindrical chamber, the exposure estimate can be read directly from a simple graduated scale, which is calibrated in milliroentgens. After use, the unit is returned to full charge (“zeroed”) by placing it in a base charging unit and charging the fiber to maximum deflection (0 mR), at which time it can be reused. These detectors have been very useful for real-time personnel exposure estimates; however, they are being rapidly replaced by solid-state personnel dosimeters.

● Geiger-Müller Detector

For a given type of radiation, the Geiger-Müller detector has a response that is independent of the energy of the event being detected owing to the gas amplification effect. However, the



a.



b.

Figure 23. (a) Photograph shows an ionization detector used for nuclear medicine surveys. (Courtesy of Keithley Radiation Measurements, Cleveland, Ohio.) (b) Photograph shows a pocket ionization detector used for real-time personnel dosimetry. The exposure can be read directly in milliroentgens from a scale, which is viewable through the opening shown on the right side of the photograph. (Courtesy of Nuclear Associates, Carle Place, NY.)

probability of detection is very energy dependent as a result of differences in stopping power at different event energies; thus, Geiger-Müller detectors are relatively inefficient for detecting x rays and gamma rays but very efficient at detecting charged particles. Although these detectors do not provide accurate indications of exposure over a broad energy range, the relatively high sensitivity (approximately a factor of 10) in comparison with that of ionization detectors makes Geiger-Müller detectors useful for radiation surveying applications in which accuracy is not essential. Nevertheless, a Geiger-Müller detector can be calibrated with a gamma emitter to provide an estimate of exposure for radiation within a limited energy range of the calibration energy. Geiger-Müller detectors have relatively long dead times (hundreds of microseconds) because they are operated in pulse mode and are not useful for surveying in high radiation fields.



a.



b.

Figure 24. Photographs show an end-window Geiger-Müller detector (a) and a Geiger-Müller detector fitted with a pancake probe (b). (Courtesy of Bicron NE, Solon, Ohio.)



Figure 25. Photograph shows an extremity and area ionization detector. This unit has a large surface area and can be handheld or wall mounted for convenient monitoring of hand contamination. (Courtesy of Nuclear Associates, Carle Place, NY.)

Figure 24 shows a Geiger-Müller detector configuration that allows different detector probes to be used for different applications. Figure 24a shows an end-window Geiger-Müller detector, which is useful for general-purpose surveys. This detector is configured with a thin entrance window to easily detect particulate radiation that might otherwise not penetrate the detector. Gamma rays penetrate the sides of the detector easily. An entrance window cap can be used to discriminate against different particulate radiation for some surveying applications. Figure 24b shows a Geiger-Müller detector fitted with a pancake probe, which is ideal for low-level surveying of

particulate radiation owing to the large surface area. This detector also has a thin entrance window for detecting low-energy beta particles. Nevertheless, this device cannot be used for detecting tritium because the betas emitted are too low in energy to penetrate the entrance window.

Geiger-Müller detectors and ionization chambers must be calibrated on an annual basis. The functioning of these devices must be checked before each use, preferably by using a check source permanently mounted on the side of the meter. In the nuclear medicine clinical setting, daily area surveys with a calibrated Geiger-Müller detector or ionization detector in every area where unsealed sources of activity are used, including the radiopharmacy, dose injection areas, and patient imaging rooms, are required by the Nuclear Regulatory Commission and state licensing agencies.

● Extremity and Area Monitor

The extremity and area monitor is a gas-filled detector with a large surface area for maximum efficiency (Fig 25). This device is operated as a proportional counter or Geiger-Müller detector to maximize detection efficiency. The device is frequently wall mounted and can be used as an area monitor or for radionuclide contamination surveying of the hands. When used as an area monitor, the device can be preset to trigger an audible alarm if activity levels exceed an arbitrary level, which is some small multiple of background counting rates. An annual efficiency test should be performed to ensure proper operation.



Figure 26. Photograph shows a nuclear medicine dose calibrator used for the assay and verification of radionuclide doses before administration to patients. The syringe containing the dose to be assayed is lowered into the center of the well-shaped containment vessel, which is filled with a high-density gas (eg, argon). The activity in millicuries or megabecquerels is read directly from the light-emitting diode readout. (Courtesy of Capintec, Ramsey, NJ.)

● Dose Calibrator

The dose calibrator is the most commonly encountered detector in the nuclear pharmacy because the Nuclear Regulatory Commission requires that all radiopharmaceutical doses be assayed before administration to patients. The dose calibrator has a well ionization chamber configuration to achieve maximum geometric efficiency. The chamber is typically filled with pressurized argon to maximize intrinsic detection efficiency. The dose calibrator does not suffer appreciably from dead time effects because it is operated in current mode; therefore, the response should be linear over the range of activities encountered clinically, which is usually 10 μCi (0.37 MBq) to 1–2 Ci (37,000–74,000 MBq). A set of precalibrated function buttons allows the user to quickly select different isotope settings (Fig 26).

Stringent quality control of dose calibrators is a requirement of the Nuclear Regulatory Commission. A radionuclide source geometric dependence test must be performed at installation and after repair. Yearly accuracy tests and quarterly linearity tests must be performed. A daily constancy test must be performed and the



Figure 27. Photograph shows a commonly encountered portable version of the scintillation well counter (seen at the base of the unit) and thyroid uptake probe (seen positioned on an extendable arm for ease of positioning). (Courtesy of Capintec, Ramsey, NJ.)

results found to be acceptable before clinical use. The accuracy and constancy of the dose calibrator must be tested with a National Institute of Standards and Technology (NIST) traceable source and must be within 10% ($\pm 5\%$) for clinical use.

■ SCINTILLATION DETECTORS

Scintillation detectors are used for counting bioassay and other radionuclide samples, measurement of thyroid uptake, and radionuclide imaging applications. Such detectors include the well counter, thyroid uptake probe, Anger scintillation camera, and PET scanner.

● Well Counter and Thyroid Uptake Probes

The scintillation well counter and thyroid uptake probe are examples of scintillation spectrometers used in nuclear medicine. The well counter is used to measure the activity concentration of in vitro blood or urine samples. The uptake probe is typically used to measure thyroid uptake of iodine-123 or iodine-131 relative to a calibrated standard capsule. These systems can be operated independently but in some cases are mounted in a portable configuration (Fig 27).

The thallium-activated sodium iodide well counter employs a well-type geometry to al-

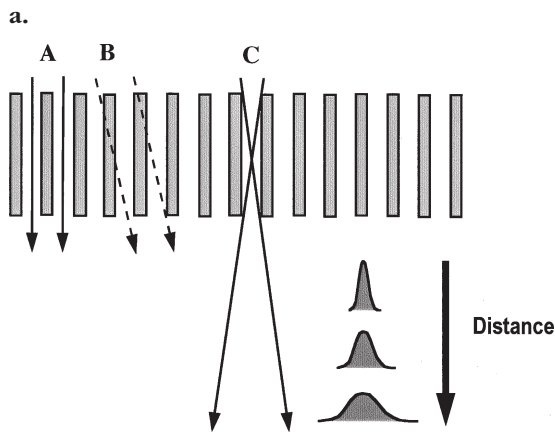
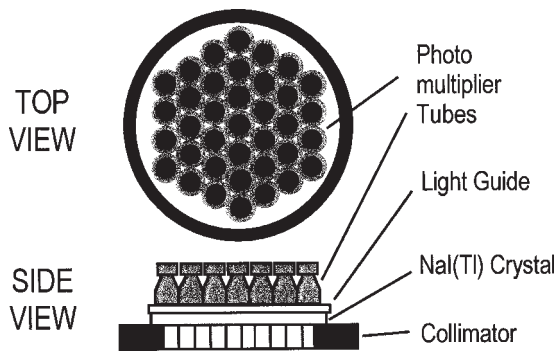


Figure 28. (a) Diagram shows a simplified schematic of the major components of the scintillation detector used for conventional radionuclide imaging. A lead collimator absorbs gamma rays traveling in directions other than parallel to the walls and channels of the collimator so that the positions and distribution of events detected in the crystal closely approximate the activity distribution in the patient. A gamma ray interaction in a thallium-activated sodium iodide crystal produces a flash of light, which is collected by an array of close-packed photomultiplier tubes. The output from the photomultipliers is fed to the electronic stage, where the signals are amplified, shaped, and fed to a position-encoding circuit (not shown) to determine the relative position of the event in the crystal and thereby form an image of the distribution of the radionuclide. (b) Diagram shows the effect of the collimator on the sensitivity and resolution of a scintillation camera. A, Gamma rays traveling parallel to the walls and channels of the collimator enter the crystal. B, Gamma rays traveling obliquely are absorbed in the lead walls of the collimator. C, Spatial resolution degrades with distance from the collimator because of the overlap in information from adjacent structures due to the wider acceptance angle with distance.

most completely surround radioactive sample sources containing very low concentrations of activity (typically 1 nCi [0.000037 MBq] to 1 μ Ci [0.037 MBq] depending on the radionuclide being counted). The well counter has a strong geometric dependence (Fig 3), and the best results

are obtained when the sample has a consistent source configuration and geometry and an activity concentration that does not induce appreciable dead time counting rate losses. The thyroid uptake probe typically employs a square, 2-inch (5-cm) diameter, 1-inch (2.5-cm) thick thallium-activated sodium iodide crystal coupled to a photomultiplier. The uptake probe also has a strong geometric dependence and must therefore be used with a consistent source-to-detector geometry to ensure accurate and reproducible results.

● Anger Scintillation Camera

The scintillation camera is a more sophisticated class of scintillation detector because events are not simply counted or sorted by energy to form a spectrum; the positions of radiation interactions in the detector are estimated to form an image of the distribution of the radionuclide.

A typical scintillation camera has a large-area thallium-activated sodium iodide crystal (typically 400 mm in diameter) in conjunction with an array of close-packed photomultiplier tubes (Fig 28a). To form an image, the detector must accept only those gamma rays traveling parallel to the axis of the detector (Fig 28b) lest the image be degraded by scattered and background radiation. A lead collimator geometrically restricts the gamma rays striking it by selectively absorbing the photons that strike obliquely (Fig 28b). The collimator is the component that most limits detection efficiency because only approximately one of every 10,000 gamma rays emitted ultimately strike the thallium-activated sodium iodide crystal. If the photon interacts in the detector, the radiation deposits the energy; this energy deposition causes a flash of scintillation photons, which are transmitted to the photomultipliers directly or through an optional light guide. The photomultiplier signals are amplified and sent to a position-encoding circuit, where the X and Y positions of the event are calculated and converted into a digital format. The summed photomultiplier output signal is used to generate a Z signal that is representative of the energy of the event. If the event energy is within the preset acceptance window, the position information is used to increment a computer memory location corresponding to the position of the event. This is the means by which the digital image is formed. Real-time persistence images are formed by feeding the X, Y, and Z analog signals to a persistence scope, which is usually mounted on the gantry of the device or the acquisition console.

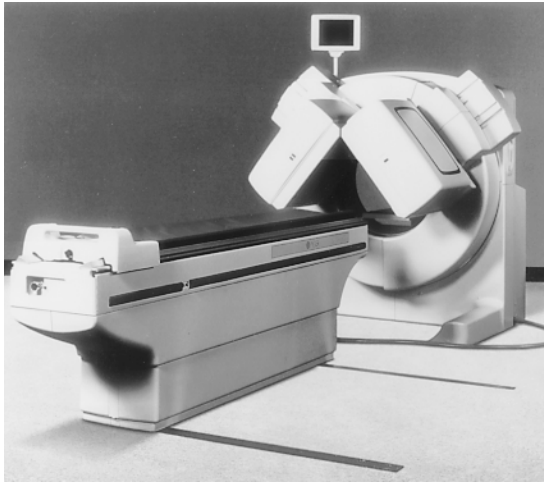


Figure 29. Photograph shows a commercial dual-headed scintillation camera. The detectors are in the orthogonal (90°) orientation favored for cardiac SPECT. A variable persistence display (shown mounted on the gantry of the device) is used to visualize the activity distribution in real time to facilitate patient positioning. (Courtesy of Picker International, Cleveland, Ohio.)

The spatial resolution of scintillation cameras degrades rapidly with distance from the collimator (Fig 28b). Therefore, care should be taken to place the collimator (ie, the detector) as close as possible to the body section being imaged.

Scintillation cameras used clinically are available in single-, double-, or triple-head configurations. Almost all scintillation cameras can be used to acquire a static planar image of the body section of interest. Scanners used in single photon emission computed tomography (SPECT) are specialized for tomographic imaging and rotate about the section being imaged. Figure 29 shows a commercial multidetector scintillation camera or SPECT scanner. This device has two opposing detectors that have been reoriented into an orthogonal orientation (90° angular separation), which is an optimal configuration for SPECT of the heart.

● PET Scanner

Radionuclide imaging of positron emitters requires a different detection scheme than that employed in conventional nuclear medicine imaging because of the requirement for increased detector stopping power at 511 keV. This stopping power can be achieved in a conventional nuclear medicine imaging device by employing a thicker ($\frac{7}{8}$ -inch [1.6-cm]) thal-

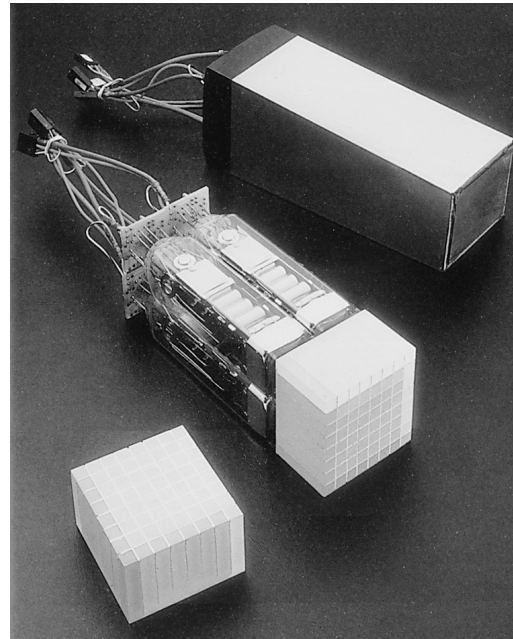


Figure 30. Photograph shows a bismuth germinate crystal and detector module. The crystal is machined with narrow channels to create 8×8 detector elements. The block is coupled to four photomultiplier tubes, which are encapsulated in one detector module. When positioned in a ring geometry (see Fig 31), these detectors can be used to image the annihilation photons produced with positron-emitting radionuclides. (Courtesy of Siemens Medical Systems, Knoxville, Tenn.)

lium-activated sodium iodide crystal with a specially designed 511-keV collimator or by employing two opposing uncollimated detectors and coincidence electronics. A typical dedicated PET imaging device uses bismuth germinate crystals due to the significantly improved stopping power of this material in comparison with that of thallium-activated sodium iodide (Table 1).

Figure 30 shows a bismuth germinate crystal and coupled photomultiplier tubes. The crystal is machined with narrow channels to create 8×8 detector elements in a single block. The effect of these channels is to promote internal reflection and minimize light spread within the crystal before detection at the photomultiplier. Four photomultiplier tubes are coupled to each bismuth germinate crystal and encapsulated in a light-tight enclosure. Because bismuth germinate is not hygroscopic, there is no need to encapsulate the crystal in a hermetically sealed containment vessel. These detector modules are mounted in a ring configuration (Fig 31). In two-dimensional PET, an image of projection data from all angles that corresponds to one transaxial section is termed a *sinogram*. In real

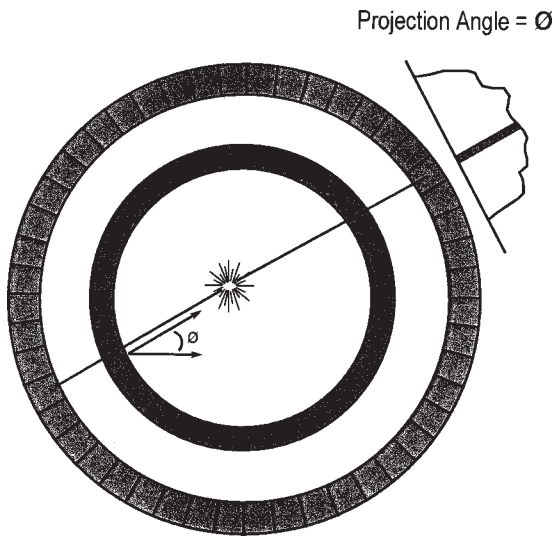


Figure 31. Diagram shows the ring detector configuration of a PET scanner. The annihilation photons produced by a positron emission are detected by an opposing detector pair. Parallel projection data are acquired by using the relative position and orientation of the detector pair.



Figure 32. Photograph shows a pocket solid-state personnel dosimeter. This unit displays cumulative exposure in milliroentgens. (Courtesy of Nuclear Associates, Carle Place, NY.)

time, the detector coincidence circuitry can determine the detector positions and coincidence chord angle to form a sinogram. Computer algorithms permit the reconstruction of a transaxial PET image from the corresponding sinogram.

■ SEMICONDUCTOR DETECTORS

Semiconductor or solid-state detectors are not as prevalent as the other types of detectors. Semiconductor detectors include personnel dosimeters, intraoperative probes, and imaging devices.



Figure 33. Photograph shows an intraoperative probe used for lymphoscintigraphy applications. The narrow tip contains a cadmium telluride wafer transducer and can be used with or without a collimator aperture sleeve, the need for which depends on the position discrimination and sensitivity required. (Courtesy of Radiation Monitoring Devices, Watertown, Mass.)

● Personnel Dosimeters

Figure 32 shows a pocket solid-state personnel monitoring device that displays cumulative exposure in milliroentgens. These personnel monitoring devices are being used more broadly and have largely replaced the pocket ionization detector for routine real-time estimation of exposure.

● Intraoperative Probes

Intraoperative probes are a class of semiconductor detectors that is becoming more prevalent in nuclear medicine practice for lymphoscintigraphy applications (Fig 33). The probes have a fine tip with a cadmium telluride or cadmium zinc telluride wafer transducer. Most devices are fitted with a removable sleeve aperture, which can improve position discrimination and accuracy with a corresponding decrease in sensitivity. Cadmium telluride has a band gap energy of 1.47 eV and an energy resolution of 2.9% at 122 keV.

● Imaging Devices

Semiconductor detectors are not commonly used in radionuclide imaging devices. At present, one semiconductor-based camera for nuclear medicine imaging is commercially available (Digirad, San Diego, Calif). However, they will be increasingly used for this purpose because of the decreasing cost, increased stopping power, and quantum detection efficiency of these detectors in comparison with those of other transducer materials.

■ SUMMARY

Radiation detectors are encountered in every aspect of nuclear medicine practice, and knowledge of the operation and function of these detectors is essential for the nuclear medicine clinician.

Detectors can be characterized in terms of function, the state of the transducer, the electronic stage, or the mode of operation. The stopping power of the transducer determines the intrinsic efficiency of the detector. The physical configuration of the detector and the relative position of a source to the transducer determine the geometric efficiency. The product of the intrinsic efficiency and the geometric efficiency is the absolute efficiency of the detector. According to the dead time characteristics of the detector, which are determined by the transducer and electronic stage, the detector may be used to detect single events (pulse mode) or to measure the rate of energy deposition (current mode). Some detectors are operated as simple counting systems by using a single-channel pulse height analyzer to discriminate against background or other extraneous events. Other detectors are operated as spectrometers and use a multichannel analyzer to form an energy spectrum. When a detector is used in this mode, the ability of the detector to accurately represent event energies can be measured by calculating the energy resolution from the FWHM of the photopeak.

Most gas-filled detectors are used as radiation surveying or monitoring instruments; however, the dose calibrator is used to assay radionuclide activity. Scintillation detectors are used primarily for counting and imaging applications because these detectors have high efficiency. Semi-

conductor detectors are encountered with greater frequency in nuclear medicine, particularly the solid-state pocket dosimeter and the intraoperative probe for lymphoscintigraphy applications. At present, one semiconductor-based camera for nuclear medicine imaging is commercially available (Digirad, San Diego, Calif). However, the decreasing costs and relatively high efficiency of solid-state detectors suggest that the next generation of nuclear medicine imaging devices will increasingly use solid-state detector technology.

Acknowledgments: The author thanks Donald Harrington, MD, chairman of the radiology department at her institution, for supporting attendance at the 1997 RSNA scientific assembly, where this material was first presented, and for his continuing support of activities related to resident education. The author also acknowledges the following companies for providing photographs or information included in this article: Bicron NE, Solon, Ohio; Capintec, Ramsey, NJ; Digirad, San Diego, Calif; Keithley Instruments, Cleveland, Ohio; Nuclear Associates, Carle Place, NY; Picker International, Cleveland, Ohio; Radiation Monitoring Devices, Watertown, Mass; and Siemens Medical Systems, PET Division, Knoxville, Tenn.

■ SUGGESTED READINGS

- Gottschalk A, Hoffer PB, Potchen EJ, eds. Diagnostic nuclear medicine. Vol 1. Baltimore, Md: Williams & Wilkins, 1988; chap 7.
- Johns HE, Cunningham JR. The physics of radiology. 4th ed. Springfield, Ill: Thomas, 1983.
- Knoll GF. Radiation detection and measurement. 2nd ed. New York, NY: Wiley, 1989.
- Rollo DF. Nuclear medicine physics, instrumentation and agents. St Louis, Mo: Mosby, 1977.
- Simmons G. The scintillation camera. Reston, Va: Society of Nuclear Medicine, 1988.
- Sorenson JA, Phelps ME, eds. Physics in nuclear medicine. 2nd ed. Philadelphia, Pa: Grune & Stratton, 1987.